

# THE EFFECT OF IMPELLER AND TANK GEOMETRY ON POWER NUMBER FOR A PITCHED BLADE TURBINE

D. CHAPPLE, S. M. KRESTA, A. WALL and A. AFACAN

*Department of Chemical and Materials Engineering, University of Alberta, Edmonton, Canada.*

Previous studies of the Rushton turbine have shown that the power number is sensitive to the details of impeller geometry, and in particular to the blade thickness, but is independent of the impeller diameter to tank diameter ratio. In this paper, a similar study is reported for the pitched blade impeller. The results show that the power number is independent of blade thickness, but dependent on the impeller to tank diameter ratio. This is exactly the opposite result to that observed for the Rushton turbine. Physical explanations are given for the differences in behaviour between the two impellers. For the Rushton turbine, power consumption is dominated by form drag, so details of the blade geometry and flow separation have a significant impact (30%) on the power number. For the pitched blade impeller, form drag is not as important, but the flow at the impeller interacts strongly with the proximity of the tank walls, so changes in the position of the impeller in the tank can have a significant impact on the power number.

*Keywords: mixing; power; torque; stirred tank; Rushton turbine; pitched blade impeller.*

## INTRODUCTION

In industrial mixing applications, the power consumption per unit volume of fluid is used extensively for scale-up, scale-down and design. In spite of its widespread use, the dependence of power consumption on impeller and tank geometry is defined only in the most general terms. This is partly due to the difficulty of obtaining accurate torque measurements on the small scale, and partly due to the predictive limitations of drag theory, particularly for recirculating three dimensional flows.

The first studies of power consumption date back to 1934<sup>1</sup>, but the early study by Rushton *et al.*<sup>2</sup> is widely cited as the first definitive work in the area. Using dimensional analysis, Rushton *et al.* developed a number of dimensionless groups, including the power number,  $N_p$ :

$$N_p = \frac{P}{\rho N^3 D^5} \quad (1)$$

where  $P$  is the power required by the impeller,  $\rho$  is the fluid density,  $N$  is the rotating speed of the impeller in rotations per second, and  $D$  is the diameter of the impeller. The power is usually calculated from measurements of the torque and the shaft speed:

$$P = 2\pi N T_q \quad (2)$$

Combining equations (1) and (2), the power number can be rewritten as:

$$N_p = \frac{2\pi T_q}{\rho N^2 D^5} \quad (3)$$

The power number is one of the most widely used design specifications in the mixing operation and has proven to be a reliable predictor of a number of process results. Given the success of the power number, the reader will rightly expect that this dimensionless group can be derived from physical fundamentals; namely a drag force analysis, or alternately an angular momentum balance. The drag force analysis which originated with White<sup>1,3</sup> is discussed in detail by Tatterson<sup>4</sup> and can be summarized as follows:

$$\begin{aligned} T_q &= \int_0^{D/2} F_D dr = \int_0^{D/2} C_D \rho \frac{V^2}{2} h r dr \\ &= 2C_D \rho h \pi^2 N^2 \int_0^{D/2} r^3 dr \propto \rho N^2 D^5 \end{aligned} \quad (4)$$

Wu and Pullum<sup>4</sup> take this approach further, and report a predictive calculation of power number using blade element theory in combination with lift and drag coefficients from the literature. They model the effects of blade angle, blade thickness, blade camber, and blade number on impeller performance. A significant limitation of this interesting theoretical approach is the assumption that there is no interaction between the impeller and the tank walls.

An alternate analysis is based on an angular momentum balance on the control volume enclosing the impeller, as shown in Figure 1. This analysis is simplified to give the power number result as follows:

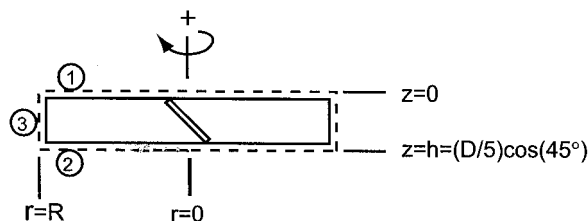


Figure 1. Control volume around the impeller.

$$T_q = \int_{\text{control surface}} \rho(\vec{V} \cdot \vec{n})(\vec{r} \times \vec{V})dA$$

$$\cong \int_{(2-1)} \rho V_z r V_{\theta} 2\pi r dr \propto \int \rho N^2 r^4 dr \propto \rho N^2 D^5 \quad (5)$$

This approach has the advantage of using velocity profiles around the impeller, so that the connection between circulation patterns and power number can be examined and the effect of geometry on power number can be better understood.

The dependence of power number on Reynolds number is analogous to well established results for the friction factor in pipe flow, and for the drag coefficient on a sphere. In the laminar range ( $Re < 10$  to  $100$ , depending on the impeller of interest), the power number is inversely proportional to the Reynolds number<sup>6</sup> ( $N_p \propto 1/Re$ ). In the fully turbulent range ( $Re > 2 \times 10^4$ ), the power number is constant and independent of the Reynolds number. The fully turbulent power number,  $N_{pft}$  or simply  $N_p$ , is often quoted as 'the' power number for a fixed impeller geometry.

In the context of the drag force grouping of the power number, many researchers have assumed that  $N_p$  depends principally on the tip speed and on the projected area of the blades. The projected area depends on variables such as impeller diameter  $D$ , blade width  $W$ , and blade length  $L$ . Bujalski *et al.*<sup>5</sup>, however, showed that blade thickness also has a significant effect on  $N_p$  for the Rushton turbine (RT). Rutherford *et al.*<sup>6</sup> confirmed this result. It has also frequently been assumed that the size of the tank is large relative to the flow around the impeller blades. This allows geometric variables involving the tank diameter, such as  $D/T$  and  $C/T$ , to be eliminated. Early studies<sup>7-9</sup> showed that  $D/T$  and  $C/T$  can affect  $N_p$  as the impeller approaches the tank walls, but results in general were contradictory and inconclusive<sup>7</sup>. Detailed studies of these effects were largely abandoned from 1975–1995, with the exception of a comprehensive paper by Medek<sup>10</sup> in 1980. More recent work by Armenante *et al.*<sup>11</sup> found a decrease in  $N_p$  with increasing  $D/T$  for the PBT. A dependence on  $C/D$  has also been reported<sup>10-12</sup>, illustrating the strong interaction between the impeller and the tank walls for the PBT impeller.

Possible variations in power number due to changes in impeller diameter, off bottom clearance, and details of the impeller construction inject a degree of uncertainty into one of the central specifications used for design of mixing equipment. Very accurate measurements of the torque and power consumption are required in order to resolve this ambiguity because at small scales the torque drops off

dramatically ( $T_q \propto D^5$ ). While the torque also increases with  $N^2$ , there are practical limits on  $N$  due to air entrainment and mechanical vibration. The difficulty of detecting the effects of  $t/D$ ,  $D/T$  and  $C/T$  on the power draw is compounded if there is a significant baseline torque due to friction. As a result, the method used to measure power draw must be carefully considered. Four experimental methods are considered here: measurement of current draw by the motor, measurement of temperature rise in the fluid, measurement of torque on the tank or motor, and use of torque transducers to measure the torque on the shaft.

King *et al.*<sup>13</sup> measured the electrical power consumed by the motor. Where the efficiency curve of the motor is known and other power losses in the system from gear boxes and bearings are both known and stable, this method was shown to work well. At the small scale, this method is difficult to apply since the additional power consumption due to the impeller is quite small relative to the total power draw.

An energy balance on the tank suggests that if the tank is insulated, the power draw can be deduced from the temperature rise of the fluid over a suitable period of time. For low viscosity fluids, the temperature rise is small, and this method is not practical. For higher viscosity fluids at low  $Re$ , reasonable results may be obtained, provided the viscosity is not a strong function of temperature. In general; however, this method is not recommended.

To measure the torque on the tank, a bearing in combination with a spring scale can be used. The 'frictionless' bearing supporting the tank is stationary once the shaft speed has stabilized, and the torque sustained by the bearing is constant. Nienow and Miles<sup>14</sup> used an 'air bearing dynamometer' for this method. Bujalski *et al.*<sup>5</sup>, whose data is referenced later in this study, also used this method. Alternately, the motor can be supported by a bearing, and the torque on the motor can be measured<sup>2</sup>. The best illustration of these arrangements is given in Figures 2–8 in Holland and Chapman<sup>15</sup>. As the impeller diameter decreases relative to the size of the tank, the inertia of the tank or motor and the frictional forces in the bearing increase relative to the torque, and this method becomes less accurate.

The most direct way to measure the torque due to fluid forces on the impeller is to measure the torque on the shaft directly. A torque transducer is installed on the shaft either outside the tank just below the motor<sup>16</sup>, or inside the tank just above the impeller<sup>17</sup>. Bujalski *et al.*<sup>5</sup>, Distelhoff *et al.*<sup>18</sup>, and Rutherford *et al.*<sup>6</sup> mounted a strain gauge on the shaft just above the impeller. An early version of this apparatus, suitable only for large torques, is shown in Nagata's<sup>3</sup> Figure 1.8. In this work, a torque transducer is installed on the shaft just below the motor. The instrument is quite fragile and calibration for very small torque measurements must be done with great care if accurate and consistent results are to be obtained.

In this paper, the sensitivity of the power number to changes in blade thickness and impeller diameter is examined for the down-pumping 45° pitched blade impeller (PBT). The experimental equipment is validated using existing data for the Rushton turbine. The range of Reynolds numbers considered extends well down into the transitional range for both the RT and the PBT. The experimental method is described here in some detail in order to encourage standardization of future work in this area.

## EXPERIMENTAL

The experiments were carried out in a 0.240 m diameter cylindrical tank with  $H=T$  as shown in Figure 2. Four rectangular baffles with a width of  $T/10$  were equally spaced around the periphery of the tank. A lid was installed to prevent air entrainment at higher impeller speeds ( $N$ ). Rushton turbines of diameter  $D=T/3$  and PBT's of diameters  $D=T/4$ ,  $T/3$  and  $T/2$  were studied. All impellers were located at an off-bottom clearance of  $C=T/3$ . Reynolds numbers from 300–150,000 were investigated, covering the range from low transitional to fully turbulent flow. Table 1 gives the properties of the test liquids and the range of Reynolds number covered by each fluid.

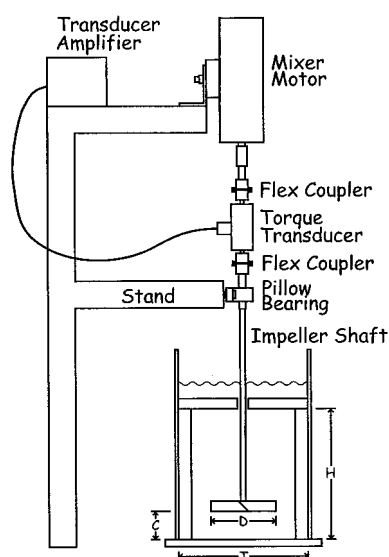


Figure 2. Schematic diagram of the experimental setup.

Scale drawings of the RT and the PBT are given in Figure 3. Detailed dimensions of all impellers are given in Table 2. The hub height of the RT was measured from the bottom of the disk to the top of the hub. The PBT's were used in the down-pumping direction. The blades were welded onto the hub or the disk and the impellers were secured at the end of the shaft using a setscrew. While some authors stabilize the shaft using a bearing at the bottom of the tank, in this work the shaft ends at the bottom of the impeller. This was done to ensure the retention of any macroinstabilities which develop below the impeller. The freedom of motion at the bottom of the shaft results in bending forces on the shaft which require some additional precautions in the installation of the torque transducer.

Figure 2 is a schematic diagram of the motor and torque transducer assembly, which is mounted on a steel framework above the tank. The mixer motor (Caframo BDC3030) can reach speeds of up to 3000 rpm and has enough power to cover the full range of the torque transducer without exceeding it. The motor speed was periodically verified using an optical tachometer. The speed remained constant to within 2% of the set speed.

The torque transducer (MCRT 3L-08T from S. Himmelstein & Co.) has a range from  $-0.7$  Nm to  $+0.7$  Nm ( $\pm 100$  oz-in). This transducer was chosen for its high precision:  $\pm 0.1\%$  of full scale. Along with this high sensitivity to torque comes a high sensitivity to bending forces and axial loads, demanding extra care and attention when mounting the transducer in the mixer assembly. A pillow bearing (see Figure 2) was placed between the torque transducer and the impeller shaft to support all of the axial, radial, and bending loads applied to the shaft due to the mixing process. This allows only the torque to be transmitted through to the torque transducer. To remove any remaining vibrations and bending forces, flex couplers were placed on either side of the transducer. These couplers also protect the transducer from small misalignments in the motor/shaft/transducer/bearing assembly. This combination

Table 1. Viscosity, density and range of  $Re$  for the three working fluids.

Liquid	Viscosity, Pa s	Density, $\text{kg m}^{-3}$	$Re$ , RT	$Re$ , PBT
TriEthylene Glycol	$4.1 \times 10^{-2}$	1120	300–2000	1000–4000
Bayol	$2.6 \times 10^{-3}$	780	9000–30,000	20,000–50,000
Water	$1.0 \times 10^{-3}$	1000	30,000–90,000	60,000–150,000

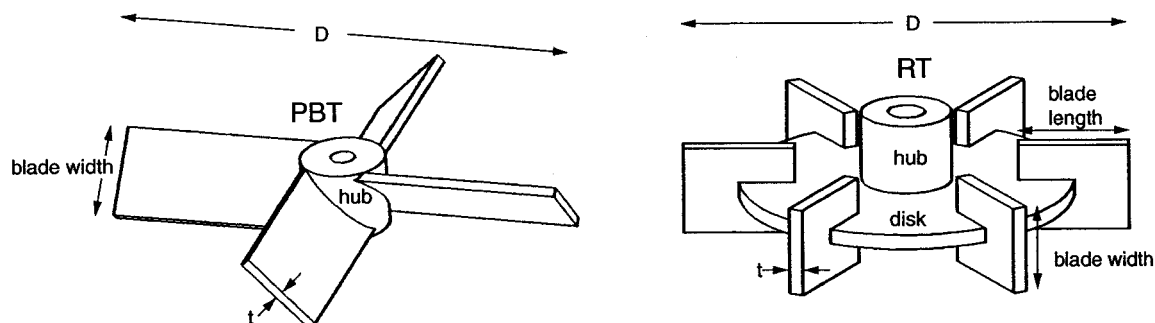


Figure 3. Scale drawings of the Pitched Blade Turbine (PBT) and the Rushton Turbine (RT).

Table 2. Impeller dimensions in millimetres.

Impeller type	T/3 RT	T/3 RT	T/3 PBT	T/3 PBT	T/3 PBT	T/3 PBT	T/4 PBT	T/2 PBT
$t/D$ (dimensionless)	0.011	0.034	0.008	0.009	0.019	0.033	0.020	0.020
Diameter, $D$	80.8	77.1	79.5	79.6	78.8	79.4	60.3	120
Hub diameter	12.8	15.4	15.9	15.9	15.9	15.9	12.7	22.2
Hub bore	6.4	6.4	6.4	6.4	6.4	6.4	6.4	6.4
Hub height	14.3	15.0	12.1	12.1	13.0	14.1	9.4	18.6
Blade thickness, $t$	0.89	2.59	0.61	0.74	1.50	2.59	1.19	2.44
Blade width	16.2	15.4	15.9	15.9	15.8	15.8	12.0	24.1
Blade length	20.1	19.3	—	—	—	—	—	—
Disk diameter	53.6	57.9	—	—	—	—	—	—
Disk thickness	1.42	2.62	—	—	—	—	—	—

of bearing and torque transducer allows measurement of torques as small as 0.03 Nm (4oz-in).

Several criteria are important for the selection of a bearing for this application. The bearing needs to absorb the axial and radial loads associated with the impellers of interest. A close clearance bearing is needed to minimize the wobble in the impeller shaft. A bearing with low friction makes it possible to measure small impeller torques accurately. An unsealed bearing will always have less friction than a sealed one, but an unsealed bearing in this orientation will leak lubricant down the shaft and into the tank. The pillow bearing selected (an INA radial sealed 1/2 inch ball bearing) is mounted in a cast iron housing which is bolted to the stand. Over time, axial loads caused the bearing to wear down, allowing increasing wobble in the shaft. The wobble increased the measured torque by as much as 5–10%. Measurements with excessive wobble were discarded and the bearing was replaced several times over the course of the study.

Figure 4 shows the dynamic response of the torque measurement to a change in  $N$ . The torque measurement can take up to 30 minutes to stabilize due to heating or cooling of the lubricant in the pillow bearing, and the resulting change in the bearing friction. In order to reduce both the bearing friction and the dynamics, temperature control was installed around the bearing. An aluminium block (0.102 m  $\times$  0.076 m  $\times$  0.050 m) was added to enclose the bearing. A thermocouple and two 125 watt electric rod heaters were used to hold the temperature of the block at

50°C. This is two degrees above the maximum temperature attained by the bearing at 1600 rpm without temperature control. A higher set point temperature would further reduce the bearing friction, but could also lead to degradation of the bearing lubricant and heating of the liquid in the tank. With temperature control, the dynamic period of the torque measurement was reduced by a factor of five and the friction in the bearing was substantially lower, as shown in Figure 4. During the experimental runs reported here, the dynamic period lasted approximately 120 seconds.

Computerized data acquisition (an Opto 22 Process I/O system and Labtech Notebook) was used to record the torque. The measured readings were filtered to remove high frequencies due to rotating imbalances and imperfections in the bearing and motor. Low pass filtering set at a threshold of 1 Hz produced an average torque which differed from the unfiltered average by less than 1%. The filtered signal was sampled at a rate of 2 Hz. This low data rate precludes examination of blade passages, macro-instabilities and turbulence.

In order to remove torques due to the pillow bearing and the shaft from the measured torque, baseline torque measurements were taken. The baseline torque was measured with the shaft in place for speeds up to 500 rpm. Above 500 rpm it was found that the viscous drag on the shaft was negligible and the shaft wobble was excessive, so the baseline measurements were done with the bearing alone. Measurements where the impeller torque was less than the baseline torque were discarded.

The torque measurements were taken over the widest possible range of rotational speeds for each geometry of interest. The dynamics were closely monitored to ensure that steady state torque measurements were obtained. At the beginning of each set of experiments, the motor was run at 800 rpm for at least half an hour. The motor was then set at the lowest speed for the run and the torque was allowed to level off. After the torque reached a constant value, the initial baseline torque was recorded, the motor stopped, the impeller added, and the motor restarted. The dynamic response for each point varied from a few minutes at the lowest speeds to an almost instantaneous response at the highest speeds. After the dynamic response died out, steady state data was collected for 60 seconds. Impeller torque measurements were taken at rotational speeds from 100 to 1700 rpm at 100 rpm intervals. Baseline measurements were taken at varying intervals as each run progressed. The intervals ranged from two baseline measurements at each of the lowest speeds to one baseline measurement for every

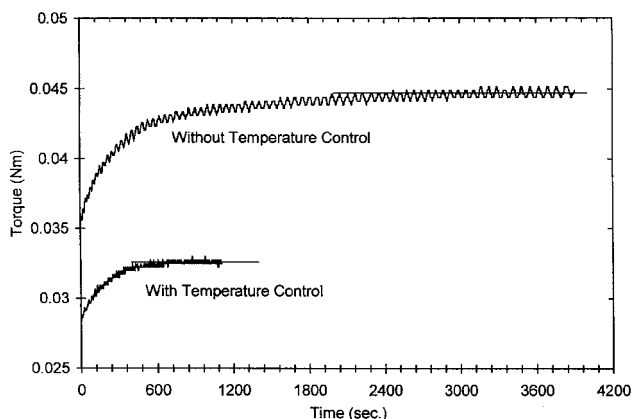


Figure 4. The effect of temperature control on the bearing baseline measurements after a change in rotational speed from 1400 to 800 rpm.

five speeds above 1000rpm, where the baseline was relatively constant.

Using the apparatus and experimental procedure described above, torque measurements were repeatable to within  $\pm 1\%$  at high speeds, and  $\pm 5\%$  at low speeds.

## RESULTS

The results are presented in two groups: the first group examines the effect of blade thickness on power number; the second the effect of  $D/T$ . In both cases, the fully turbulent power number ( $N_{pft}$ ) is used to provide an overall perspective, followed by more detailed results showing the variation of power number with Reynolds number.

Bujalski *et al.*<sup>5</sup> and Rutherford *et al.*<sup>6</sup> refer to  $N_{pft}$  as the mean peak power number. Bujalski *et al.*<sup>5</sup> first defined  $N_{pft}$  as the average of the power numbers measured from  $Re = 20,000$  to twice the Reynolds number where surface aeration is first observed. Bujalski *et al.*<sup>5</sup> also corrected  $N_{pft}$  for variations in blade width. In this study, a lid on the tank was used to prevent surface aeration, although mechanical vibrations and the range of the torque transducer limited the attainable  $Re$  to a similar level. Blade width correction was not necessary since all impeller blades were within  $\pm 0.5\%$  of  $W = D/5$ . In this work,  $N_{pft}$  is defined as the average of all  $N_p$  measurements for  $Re > 20,000$ .

Figure 5 shows the effect of  $t/D$  on the fully turbulent power number for the RT and the 4-bladed PBT. The agreement between the RT results from three different laboratories is extremely good: all three show a variation of 30% in the power number over the range of  $t/D$ 's considered. The second significant result from Figure 5 is that the power number is independent of  $t/D$  for the PBT. While the blade thickness is varied by a factor of three, the power number is essentially constant. This suggests that the thickness of the blade affects the details of flow separation and trailing vortex formation for the RT, while for the more streamlined PBT, flow separation is less dominant and skin drag plays a more important role. It is widely accepted that the trailing vortices for the PBT are much weaker and more meandering than those for the RT, providing further support for the relative importance of flow separation for the two impellers.

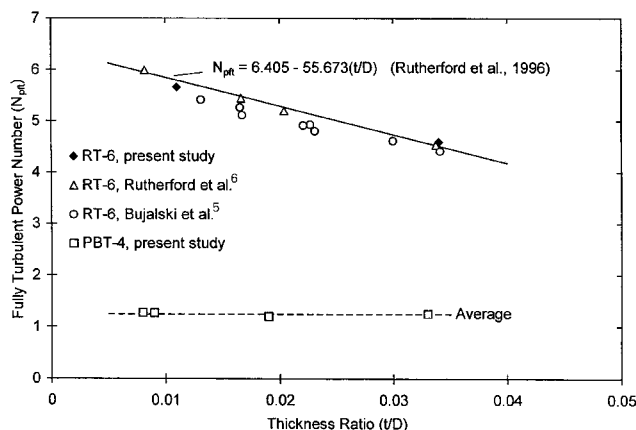


Figure 5. Effect of blade thickness ratio on fully turbulent power number for a six bladed Rushton Turbine and a down-pumping four bladed  $45^\circ$  pitched blade turbine.

The experimental results for the RT are expanded in Figure 6, where the power number is given as a function of  $Re$ . Considering first the agreement between the two studies shown, the  $t/D = 0.034$  and  $t/D = 0.0337$  data are in very close agreement, and the  $t/D = 0.011$  data set follows the previously established trend from Rutherford *et al.*<sup>6</sup>. While the average power number,  $N_{pft}$  is reported in Figure 5, Figure 6 shows that the power number for the RT is not constant from  $2 \times 10^4 < Re < 7 \times 10^4$ . In fact, the variation with Reynolds number for a single impeller and blade thickness is of the same order of magnitude as the variations in  $N_{pft}$  due to blade thickness. This result agrees closely with data reported by Rutherford *et al.*<sup>6</sup>, Distelhoff *et al.*<sup>18</sup> and Ibrahim and Nienow<sup>12</sup>. New data from this study shows that the effect of  $t/D$  extends well into the transitional regime over another two orders of magnitude of  $Re$ . A similar effect was observed by Magelli<sup>19</sup>, who observed that the effect of disk thickness is significant for  $500 < Re < 20,000$  and disappears around  $Re = 50$ , with the laminar regime beginning at  $Re = 10$ . Returning to the analogy with pipe flow and friction factors, the effect of geometry on power number (and friction factor) persists at lower Reynolds numbers, but is less significant as the Reynolds number drops.

Figure 7 reinforces the contrast between the behaviour of the power number for the RT and the PBT. The scale on Figure 7 is adjusted so that the range of the y-axis is one and a half  $N_{pft}$ , providing a consistent basis for comparison with Figure 6 for the RT. The only variation in the data is for the  $t/D = 0.019$  impeller. A closer examination of these blades revealed rounded edges, which would reduce the profile drag and the power number, explaining the small variation in the results. Aside from this deviation, there is no discernable difference between the four PBT impellers with different  $t/D$  ratios, and there is no significant variation of  $N_p$  with Reynolds number for  $Re > 2 \times 10^4$ . In this case, the average  $N_{pft}$  reflects the data very well. It can be concluded that  $N_{pft}$  is not sensitive to blade thickness for the PBT impeller.

Moving to the effect of  $D/T$ , Figure 8 shows a 15% change in  $N_{pft}$  due to variations in  $D/T$  for the PBT. All of this data is taken at  $C = T/3$ , as measured from the lower edge of the impeller blades. Figure 9 shows that the difference in power number is larger than the variance in

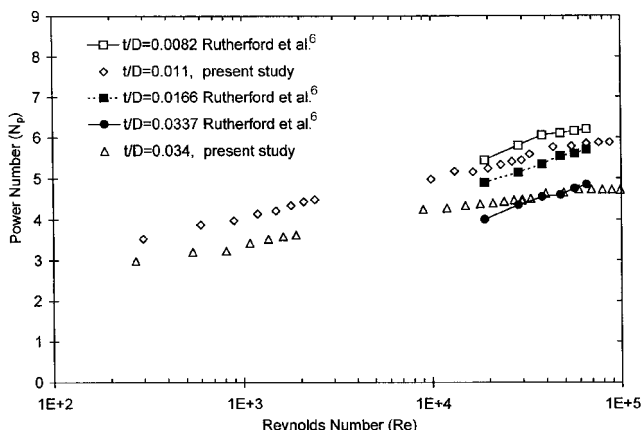


Figure 6. Variation of power number with Reynolds number for a range of impeller thickness ratios for a six bladed Rushton Turbine.

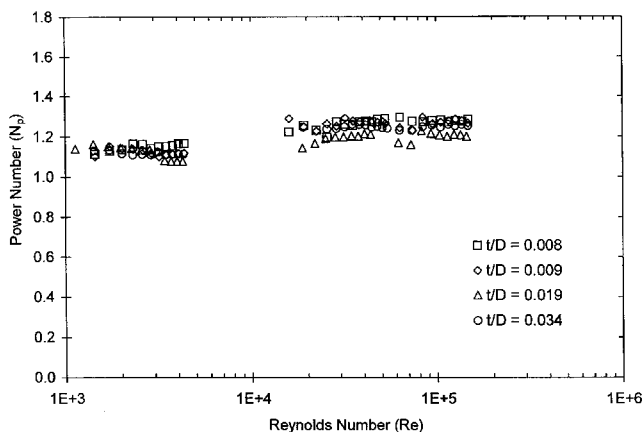


Figure 7. Variation of power number with Reynolds number for a range of impeller thickness ratios for a down-pumping four bladed 45° pitched blade impeller ( $D = T/3$ ,  $T = 240$  mm).

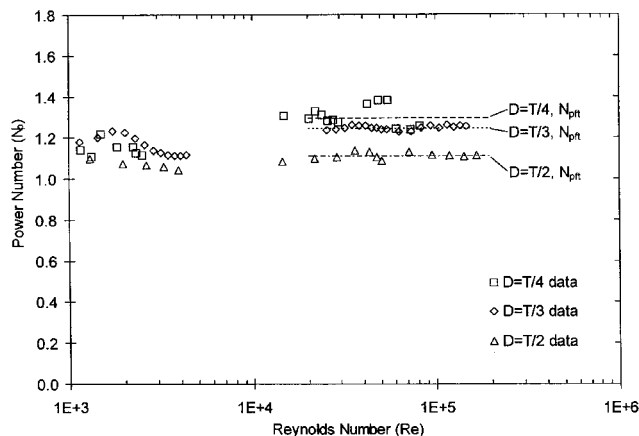


Figure 9. Variation of power number with Reynolds number for three diameters of down-pumping four bladed 45° pitched blade impellers ( $T = 240$  mm,  $C = T/3$ ).

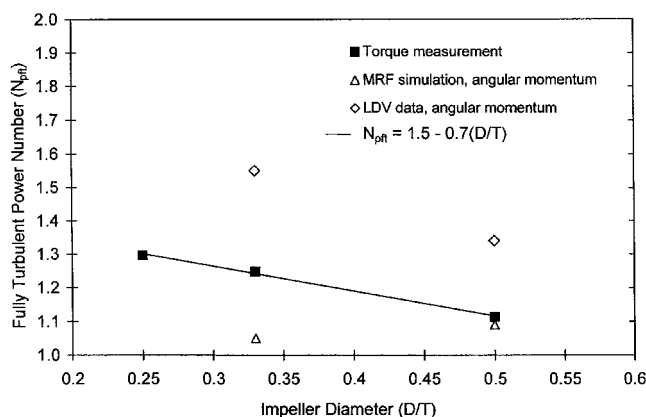


Figure 8. Effect of impeller diameter on the fully turbulent power number of down-pumping four bladed 45° pitched blade impellers ( $T = 240$  mm,  $C = T/3$ ).

the fully turbulent data. The relatively large variation in the  $D = T/4$  data set is due to shaft vibration at the higher  $N$  required for this small impeller. To obtain more data, the allowable variability in the measurements was increased by allowing measured torques less than the baseline torque down to as low as half the baseline measurement. All of the data is within a 95% confidence limit above  $Re = 2 \times 10^4$ . This result is contrasted with studies by Ibrahim and Nienow<sup>12</sup>, Rutherford *et al.*<sup>6</sup> and Bujalski *et al.*<sup>1</sup> all of which showed no effect of  $D/T$  on  $N_p$  for the RT for  $0.33 < D/T < 0.5$ . While the PBT power draw is much less sensitive to details of the impeller geometry than the RT, Figures 8 and 9 show that it is much more sensitive to interactions with the tank walls.

Interactions between the PBT and the tank walls result in changes in the velocity field in the tank, as reported by Kresta and Wood<sup>20</sup>. Through the use of an angular momentum balance, velocity profiles were used to explore the effect of  $D/T$  on  $N_{pft}$  in terms of the velocity field around the impeller. Applying an angular momentum balance to the control volume in Figure 1 results in equation (6):

$$T_q = 2\pi\rho \left[ \int_0^R (V_{z2}V_{\theta2})r^2 dr - \int_0^R (V_{z1}V_{\theta1})r^2 dr + R^2 \int_0^{z=(D/5)\cos(45^\circ)} V_{r3}V_{\theta3} dz \right] \quad (6)$$

Velocity profiles on the surface of the control volume around the impeller were determined for a  $T = H = 0.24$  m flat-bottomed tank with water as the working fluid. Results from both laser Doppler velocimetry (LDV) and computational fluid dynamics (CFD) are shown in Figure 10. The CFD simulations (fully described in<sup>21</sup>) were performed in the Fluent multiple reference frame (MRF) realization with the  $k-\varepsilon$  turbulence model, a grid of (50 tangential  $\times$  40 radial  $\times$  71 axial) cells, and convergence of all normalized residuals to less than  $5 \times 10^{-4}$ . The MRF realization fixes the impeller at one position relative to the baffles, thus neglecting the impact of the motion between the impeller and the baffles on the mean flow. The LDV experiments (fully described in<sup>22</sup>) were done in forward scatter mode with velocity profiles taken 3 mm from the impeller blades. Data was collected at each point for one minute to ensure a stable mean velocity. There was no evidence of velocity biasing. With one exception, the axial velocity close to the blade tips on the lower surface of the impellers, the agreement between velocity profiles is extremely good. Where LDV measurements could not be obtained (the angular velocity at the tip of the blades) the CFD data was used to calculate the torque and power number. The results are shown in Figure 8.

The results of this analysis illustrate clearly the sensitivity of the angular momentum analysis, and the difficulties inherent in this approach. The variations in power number calculated from angular momentum are dominated by the axial velocity profile at the lower edge of the impeller (surface 2). Where the CFD result underpredicts  $N_{pft}$  for the  $D = T/3$  impeller, it also underpredicts the axial velocity profile. When the LDV based power number drops from  $D = T/3$  to  $D = T/2$ , it is as a result of a drop in the axial velocity profile. This change in the velocity profile for the larger impeller gives a reduced pumping capacity, effectively

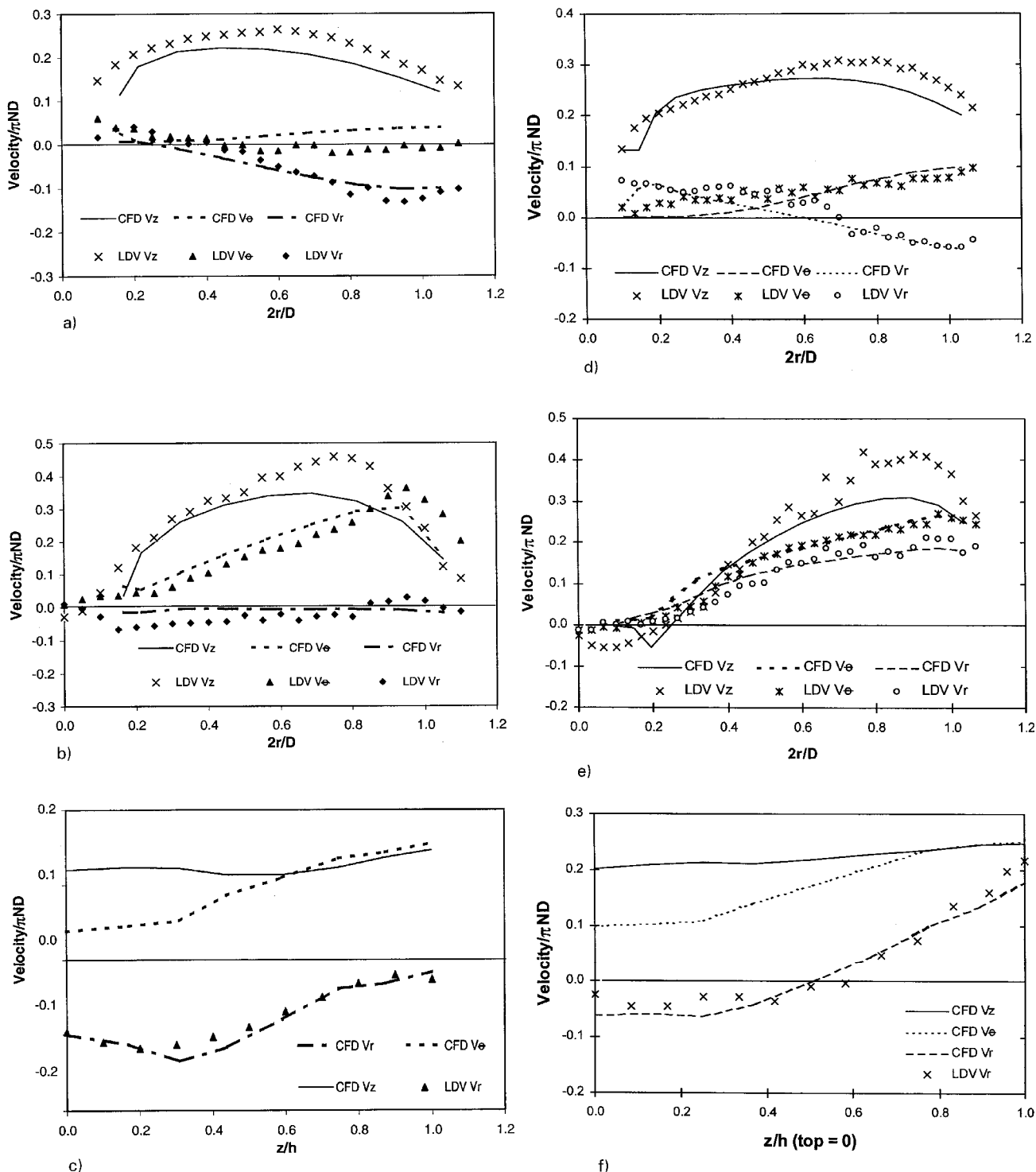


Figure 10. Velocity profiles over the control surface illustrated in Figure 1 for the  $D=T/3$  impeller (a) surface 1, the top; (b) surface 2, the bottom; (c) surface 3 the tip of the blades; and for the  $D=T/2$  impeller (d) surface 1, the top; (e) surface 2, the bottom; (f) surface 3, the tip of the blades.

reducing the mass flowrate in the angular momentum balance. Thus, while the results are not completely satisfying from a quantitative point of view, they do provide a better physical explanation for the change in power number.

Armenante *et al.*<sup>11</sup> and Medek<sup>10</sup> also found a decrease in  $N_p$  with increasing  $D/T$  for the PBT. Medek shows results for 3 and 6 bladed impellers which agree with the torque

measurements in Figure 8, and cover a wider range of  $D/T$  ratios. Returning to the analogy with friction factors in pipe flow, Figure 9 shows that the effect of  $D/T$  on power number decreases as the  $Re$  is reduced to the low transitional range. Once again, the effect of geometry becomes less important as the Reynolds number drops and the viscous forces become significant.

## CONCLUSIONS

This work compares the importance of impeller and tank geometry for two widely used impellers. For the Rushton turbine, power consumption is dominated by form drag, so details of the blade geometry and flow separation have a significant impact (30%) on the power number. For the PBT, form drag is not as important, but the flow at the impeller interacts strongly with the proximity of the tank walls, so changes in the position of the impeller in the tank can have a significant impact on the power number (15%) due to changes in the flow patterns. For both impellers, the importance of geometry decreases as the Reynolds number drops into the transitional regime and viscous forces come into play.

From the data presented in this paper, it is concluded that:

- (1) Accurate torque measurement techniques have been established and documented. Results from three different labs are compared, and are in very close agreement. This level of accuracy goes a step beyond the classical results, which established generic power number curves for many standard impellers.
- (2) For pitched blade impellers at  $Re > 2 \times 10^4$ , the power number is constant and  $N_{pft}$  is an accurate representation of the data. For the Rushton turbine, there are changes in  $N_p$  even above the nominal limit of  $2 \times 10^4$ .
- (3) There is no effect of blade thickness on power number for the 4-bladed PBT impeller. The previously reported effect of blade thickness for the RT was replicated, and the curves extended down into the transitional regime.
- (4) The fully turbulent power number for the 4-bladed PBT impeller is a function of  $D/T$ . The variation is linear for the data collected here, with  $N_{pft} = 1.5 - 0.7(D/T)$  for  $(0.25 < D/T < 0.5)$  at  $C = T/3$ .

The angular momentum balance set out in equation (6) provides a way to understand variations in power number as various aspects of impeller and tank geometry are changed. This analysis, however, is extremely sensitive and does not yield quantitatively satisfying results for either LDV or CFD measurements.

## NOMENCLATURE

$A$	area of control surface, $m^2$
$C$	off bottom clearance of the impeller, m
$C_D$	drag coefficient
$D$	diameter of the impeller, m
$F_D$	drag force, N
$h$	projected blade height, m
$H$	tank height, m
$L$	blade length, m
$N$	rotational speed of the impeller, rpm
$N_{pft}$	fully turbulent power number
$N_p$	power number
$\bar{n}$	unit normal vector at control volume surface
$P$	power, W
$r$	radius or radial coordinate when used as a subscript, m
$R$	radius of the impeller, m
$Re$	Reynolds number $Re = \rho ND^2/\mu$
$T$	tank diameter, m
$t$	blade thickness, m
$T_q$	torque, Nm
$V$	fluid velocity, $m s^{-1}$
$W$	blade width, m
$z$	axial coordinate, m

## Greek symbols

$\mu$	viscosity, Pa s
$\theta$	tangential direction
$\rho$	liquid density, $kg m^{-3}$

## Acronyms

PBT	pitched blade turbine
RT	Rushton turbine

## REFERENCES

1. Uhl, V. W. and Gray, J. B., 1966, *Mixing, Theory and Practice*, vol. 1 (Academic Press, New York, USA), pp 120.
2. Rushton, J. H., Costich, E. W. and Everett, H. J., 1950, Power characteristics of mixing impellers, *Chem Eng Prog*, 46(8): 395–476.
3. Nagata Shinjie, 1975, *Mixing Principles and Applications* (John Wiley and Sons, New York, USA), pp 13.
4. Wu, J. and Pullum, L., 2000, Performance analysis of axial-flow impellers, *AIChE J*, 46(3): 489–498.
5. Bujalski, W., Nienow, A. W., Chatwin, S. and Cooke, M., 1987, The dependency on scale of power numbers of Rushton disc turbines, *Chem Eng Sci*, 42(2): 317–326.
6. Rutherford, K., Mahmoudi, S. M. S., Lee, K. C. and Yianneskis, M., 1996, The influence of Rushton impeller blade and disk thickness on the mixing characteristics of stirred vessels, *Trans IChemE, Part A, Chem Eng Res Des*, 74(A3): 369–378.
7. Bates, R. L., Fondy, P. L. and Corpstein, R. R., 1963, An examination of some geometric parameters of impeller power, *I and EC Proc Des Dev*, 2(4): 310–314.
8. Nienow, A. W. and Miles, D., 1971, Impeller power numbers in closed vessels, *I and EC Proc Des Dev*, 10(1): 41–43.
9. Gray, D. J., Treybal, R. E. and Barnett, S. M., 1982, Mixing of single and two phase systems: Power consumption of impellers, *AIChE J*, 28(2): 195–199.
10. Medek, J., 1980, Power characteristics of agitators with flat inclined blades, *Inter Chem Eng*, 20: 664–672.
11. Armenante, P. M., Mazzarotta, B. and Chang, G., 1999, Power consumption in stirred tanks provided with multiple pitched-blade turbines, *Ind Eng Chem Res*, 38(7): 2809–2816.
12. Ibrahim, S. and Nienow, A. W., 1995, Power curves and flow patterns for a range of impellers in Newtonian fluids:  $40 < Re < 5 \times 10^5$ , *Trans IChemE, Part A, Chem Eng Res Des*, 73(A4): 485–491.
13. King, R. L., Hiller, R. A. and Tattersson, G. B., 1988, Power consumption in a mixer, *AIChE J*, 34(3): 506–509.
14. Nienow, A. W. and Miles, D., 1969, A dynamometer for the accurate measurement of mixing torque, *J Sci Instrum*, 2(2): 994–995.
15. Holland, F. A. and Chapman, F. S., 1966, *Liquid Mixing and Processing in Stirred Tanks* (Reinhold Pub Corp, New York, USA), pp 46.
16. Raidoo, A., Raghava Rao, K. S. M. S., Sawant, S. B. and Joshi, J. B., 1987, Improvements in gas inducing impeller design, *Chem Eng Comm*, 54: 241–246.
17. Kuboi, R., Nienow, A. W. and Allsford, K., 1983, A multipurpose stirred tank facility for flow visualization and dual impeller power measurement, *Chem Eng Comm*, 22: 29–40.
18. Distelhoff, M. F. W., Laker, J., Marquis, A. J. and Nouri, J. M., 1995, The application of a strain gauge technique to the measurement of the power characteristics of five impellers, *Experiments in Fluids*, 20: 56–58.
19. Magelli, F., 2001, *Personal Communication*.
20. Kresta, S. M. and Wood, P. E., 1993, The mean flow field produced by a  $45^\circ$  pitched blade turbine: Changes in the circulation pattern due to off bottom clearance, *Can J Chem Eng*, 71: 42–52.
21. Bhattacharya, Sujit and Kresta, S. M., 2001, CFD simulations of three-dimensional wall jets in a stirred tank, *Can J Chem Eng.*, in press.
22. Zhou, Genwen, and Kresta, S. M., 1996, Distribution of energy between convective and turbulent flow for three frequently used impellers, *Trans IChemE, Part A, Chem Eng Res Des*, 74(A3): 379–389.
23. Tattersson, G. B., 1991, *Fluid Mixing and Gas Dispersion in Agitated Tanks* (McGraw-Hill, Inc, USA).

## ACKNOWLEDGEMENTS

The authors gratefully acknowledge the financial support of Caframo Ltd. and Lightnin. The LDV measurements were carried out by Patricia

Comeau and Vesselina Roussinova. Sujit Bhattacharya provided the CFD simulation results.

city of Alberta, Edmonton, T6G 2G6, Canada.  
E-mail: suzanne.kresta@ualberta.ca

### ADDRESS

Correspondence concerning this paper should be addressed to Professor S. M. Kresta, Department of Chemical and Materials Engineering, Univer-

*The manuscript was communicated via our International Editor for Canada, Professor P. Tanguy, 16 January 2001, and was accepted for publication after revision 4 February 2002.*